
ELSEVIER

Journal of Computational and Applied Mathematics 140 (2002) 673–693

JOURNAL OF COMPUTATIONAL AND APPLIED MATHEMATICS

www.elsevier.com/locate/cam

On the adjacencies of triangular meshes based on skeleton-regular partitions

Angel Plaza[a,*], María-Cecilia Rivara[b]

[a] *Department of Mathematics, University of Las Palmas de Gran Canaria, 35017-Las Palmas de Gran Canaria, Canaria, Spain*

[b] *Department of Computer Science, University of Chile, Santiago, Chile*

Received 18 September 2000; received in revised form 31 March 2001

Abstract

For any 2D triangulation τ, the 1-skeleton mesh of τ is the wireframe mesh defined by the edges of τ, while that for any 3D triangulation τ, the 1-skeleton and the 2-skeleton meshes, respectively, correspond to the wireframe mesh formed by the edges of τ and the "surface" mesh defined by the triangular faces of τ. A skeleton-regular partition of a triangle or a tetrahedra, is a partition that globally applied over each element of a conforming mesh (where the intersection of adjacent elements is a vertex or a common face, or a common edge) produce both a refined conforming mesh and refined and conforming skeleton meshes. Such a partition divides all the edges (and all the faces) of an individual element in the same number of edges (faces). We prove that sequences of meshes constructed by applying a skeleton-regular partition over each element of the preceding mesh have an associated set of difference equations which relate the number of elements, faces, edges and vertices of the nth and $(n-1)$th meshes. By using these constitutive difference equations we prove that asymptotically the average number of adjacencies over these meshes (number of triangles by node and number of tetrahedra by vertex) is constant when n goes to infinity. We relate these results with the non-degeneracy properties of longest-edge based partitions in 2D and include empirical results which support the conjecture that analogous results hold in 3D.

MSC: 51M20; 52B10

Keywords: Partitions; Adjacencies; Triangular and tetrahedral meshes

1. Introduction

The *kissing number* of a convex body K is the maximum number of congruent copies of K that can touch K without overlapping with each other. For instance, the kissing number of the 2D ball B^2 is 6. The question about the number for the 3D ball B^3 caused a dispute between Isaac Newton and

* Corresponding author.

E-mail addresses: aplaza@dma.ulpgc.es (A. Plaza), mcrivara@dcc.uchile.cl (M.-C. Rivara).

0377-0427/02/$ - see front matter
PII: S0377-0427(01)00484-8

David Gregory. Newton conjectured that the answer was 12 while Gregory thought 13 was possible. It took 180 years before the question was answered: Hoppe proved that Newton was right [17]. Perhaps for this reason the kissing number of a convex body K is also known as the *Newton number* of K.

In addition, in the field of numerical methods (specially related with finite element methods) a considerable effort has been done in the last 20 years for designing and implementing algorithms both for the generation and the refinement of quality meshes [9]. In this context, several mesh smoothing and mesh improvement techniques have been developed and used [10,15]. Several topological and geometrical regularity measures for simplices (triangles in 2D, tetrahedra in 3D) as well as for simplicial grids (*triangulations*) have been also proposed in literature [11,29]. In particular, Shimada [29] proposed the following quality measure for a triangulation τ:

$$\varepsilon_\tau = \frac{1}{n}\sum_{i=1}^{n} |\delta_i - D|, \tag{1}$$

where δ_i represents the *degree* of node i (the number of nodes connected to the ith interior node), $D=6$ for triangles, and $D=12$ for tetrahedra, and n is the total number of interior nodes in the domain. Note, that by using the ε_τ measure, as the elements become more equilateral, the mesh irregularity approaches 0, but vanishes only when all the nodes have D neighbors, a rare situation. Otherwise, it has a positive value that quantifies how much the mesh differs from a perfectly regular triangular lattice. Recently, Buss and Simpson have proved that planar mesh refinement cannot be both local and regular [8], and in higher dimensions it is well-known that there is not a regular simplicial partition of the space.

In this paper, we consider skeleton-regular partitions of simplices, which are partitions that divide each topological element of the same dimension—edges and faces—in the same number of son-elements. For any input mesh τ_0 we study the asymptotic behavior of the average of the degree of the nodes when the partition is iteratively and globally used to produce a sequence of conforming meshes.

The paper is organized as follows. In Section 2, some definitions and notations are introduced. In Sections 3 and 4, skeleton-regular partitions in two and three dimensions are, respectively, discussed. In Section 5, the asymptotic average of the adjacencies of the topological elements are studied for both 2- and 3D cases. Section 6 includes numerical experiments with the 8T-LE partition and a comparison with the adjacency numbers of practical meshes used in finite element calculations. Some concluding remarks are included in Section 7.

2. Definitions and notations

Some previous definitions and notations are summarized here.

Definition 2.1 (*simplex*). A closed subset $T \subset \mathbb{R}^n$ is called a (k)-*simplex*, $0 \leqslant k \leqslant n$ if T is the convex linear hull of $k+1$ vertices $x^0, x^1, \ldots, x^k \in \mathbb{R}^n$

$$T = [x^{(0)}, x^{(1)}, \ldots, x^{(k)}] := \left\{ \sum_{j=0}^{k} \lambda_j x^{(j)} \;\middle|\; \sum_{j=0}^{k} \lambda_j = 1,\ \lambda_j \in [0,1],\ 0 \leqslant j \leqslant k \right\}. \tag{2}$$

If $k=n$ then T is simply called *simplex* or *triangle* in $\mathbb{R}^n$. In what follows (2)-simplices and (3)-simplices are also called triangles and tetrahedra respectively.

Definition 2.2 (*conforming triangulation*). Let Ω be any bounded domain in $\mathbb{R}^2$, or $\mathbb{R}^3$ with no-empty interior and polygonal boundary $\partial\Omega$, and consider a partition of Ω into a set of triangles $\tau = \{t_1, t_2, t_3, \ldots, t_n\}$. Then we say that τ is a conforming triangulation if the following properties hold:

1. $\Omega = \bigcup t_i$,
2. $\text{interior}(t_i) \neq \emptyset$, $\forall t_i \in \tau$,
3. $\text{interior}(t_i) \cap \text{interior}(t_j) = \emptyset$, if $i \neq j$,
4. $\forall t_i, t_j \in \tau$ with $t_i \cap t_j \neq \emptyset$, then $t_i \cap t_j$ is an entire face or a common edge, or a common vertex.

Definition 2.3 (*k-face*). Let $T = [x^{(0)}, x^{(1)}, \ldots, x^{(n)}]$ be an (n)-simplex in $\mathbb{R}^n$. A k-simplex $S = [y^{(0)}, y^{(1)}, \ldots, y^{(k)}]$ is called a (k)-*subsimplex* or a (k)-*face* of T if there are indices $0 \leqslant i_0 < i_1 < \cdots i_k \leqslant n$ such that $y^{(j)} = x^{(i_j)}$ for $0 \leqslant j \leqslant k$.

Obviously, the (0)- and (1)-face of T are just its vertices and edges, respectively.

Definition 2.4 (*skeleton*). Let τ be any nD ($n=2$ or 3) conforming triangular mesh. The *k-skeleton* of τ is the union of its k-faces. The $(n-1)$-skeleton is also called the skeleton [6].

Note that the skeleton of a tetrahedral mesh in 3D is a "surface mesh" defined by the faces of the elements (tetrahedra) of the volume mesh; while in 2D the skeleton of a mesh is a wireframe mesh defined by the set of the edges of the triangles. Note that by extension the n-skeleton of a triangulation τ is the triangulation itself. Thus the skeleton can be understood as a new triangulation: if τ is a 3D conforming triangulation in $\mathbb{R}^3$, $skeleton(\tau)$ is a surface triangulation embedded in $\mathbb{R}^3$. Furthermore, if τ is conforming, then $skeleton(\tau)$ is also conforming.

Definition 2.5 (*skeleton-regular partition*). For any triangle or tetrahedron t, a partition of t will be called *skeleton-regular* if the following properties hold:

1. All the topological elements of the same dimension, that is all the elements of the k-skeleton ($0 \leqslant k \leqslant n$) are subdivided in the same number of son-elements.
2. The application of the partition to each individual element in any conforming mesh produces a conforming triangulation.

In order to illustrate this concept, consider Fig. 1 where a single triangle t_0 has been divided into 9 triangles by using a 2D skeleton-regular partition which consists on adding one interior node and two nodes over each edge of t_0, and then joining the interior node with every boundary vertex and node. Note that in this case each edge was divided in 3 equal parts and the triangle itself is partitioned into 9 triangles. More examples in 2- and 3D are considered in next sections.

Remark 2.1. Note that the iterative application of any skeleton-regular partition over any conforming triangulation produces a sequence of finer and nested conforming triangulations.

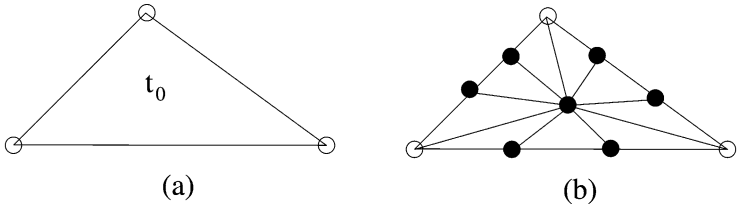

Fig. 1. Example of 2D skeleton-regular partition.

3. Skeleton-regular partitions in 2D

In this section we review some triangle partitions in 2D, and for those which are skeleton-regular partitions we study their associated recurrence equations (the constitutive equations of the globally refined meshes).

In order to introduce the 4-triangles longest-edge partition the following (non-skeleton-regular) partition is needed [22]:

Definition 3.1 (*edge bisection and longest-edge bisection*). The longest-edge bisection of a triangle is the bisection of t by the midpoint of the longest-edge and its opposite vertex (see Fig. 2(a)). If the chosen midpoint is not the longest-edge midpoint then it is said that a simple bisection has been performed (see Fig. 2(b)).

Definition 3.2 (*the* 4-*triangles longest-edge* (4*T-LE*) *partition*). The triangle is bisected by its longest edge, followed by the edge bisection of the resulting triangles by the remaining original edge of t (see Fig. 3(a)).

Definition 3.3 (*the* 4-*triangles similar partition*). The triangle is divided into four similar triangles by connecting the edge midpoints by means of line segments parallel to the edges of t (Fig. 3(b)).

Definition 3.4 (*the* 4-*triangles shortest-edge partition*). This partition divides the triangle into four triangles in such a way that a first shortest-edge bisection of the initial triangle is performed, followed by simple bisection of the resulting triangles by the remaining edges of t (Fig. 3(c)).

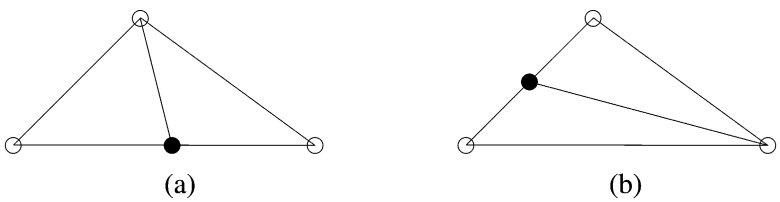

Fig. 2. (a) Longest-edge bisection of t; (b) simple bisection of t.

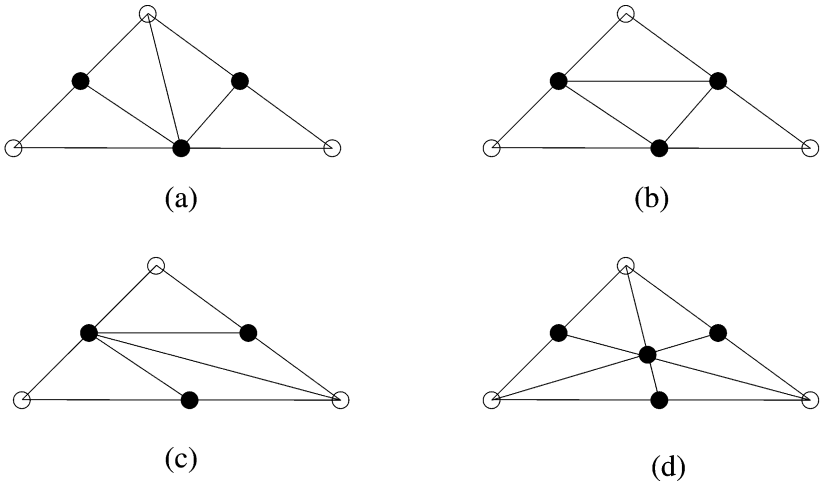

Fig. 3. Skeleton-regular partitions in 2D: (a) 4 triangles longest-edge partition of t_0; (b) 4 triangles similar partition; (c) 4 triangles shortest edge partition; (d) baricentric partition.

Proposition 3.1. *Let τ_0 be any initial conforming triangulation with N_0 vertices, E_0 edges and T_0 triangles. Then, after n applications of either the 4 triangles longest-edge partition or the 4 triangles similar partition, or the 4 triangles shortest edge partition to each triangle of τ_0 and its descendants, producing a globally refined and conforming triangulation τ_n, the number of nodes, edges and triangles in τ_n (respectively, N_n, E_n and T_n) are related with the number of elements in the preceding triangulation τ_{n-1} by means of the following constitutive equations*:

$$\begin{aligned} N_n &= N_{n-1} + E_{n-1}, \\ E_n &= 2E_{n-1} + 3T_{n-1}, \\ T_n &= 4T_{n-1}. \end{aligned} \tag{3}$$

Longest-edge partitions have been studied by Rivara and co-workers (see, for instance [22–28]). Longest-edge based partitions and algorithms in 2D have the following important non-degeneracy property:

Theorem 3.1. *The iterative use of either the longest-edge partition or the 4-triangles longest-edge partition over any triangle t and its descendants only produces triangles whose smallest interior angles are always greater than or equal to $\alpha/2$, where α is the smallest interior angle of the initial triangle. Furthermore, this result also extends for the triangulation refinement algorithms based on these partitions.*

Moreover, when the 4T-LE partition is iteratively applied over any initial obtuse triangle, the following improved results hold [24]:

Theorem 3.2. *Let t_0 be any obtuse triangle of smallest angle α_0 and largest angle γ_0. Then*:
(1) *The* 4*-triangles longest-edge partition of t_0 produces one similarly distinct triangle t_1 (of smallest angle α_1 and largest angle γ_1) such that $\alpha_1 \geqslant \alpha_0$ and $\gamma_1 \leqslant \gamma_0 - \alpha_1$ (see Fig.* 3(a)).
(2) *The* 4*-triangles longest-edge partition of any obtuse triangle t_0 and its descendants produces a finite sequence of N improved similarly distinct triangles t_i of largest angle γ_i, and smallest angle α_i such that*
   (a) *t_i is obtuse for $i = 1, 2, \ldots, N-1$, and t_N is non-obtuse,*
   (b) *$\alpha_j \geqslant \alpha_{j-1}$ for $j = 1, 2, \ldots, N$,*
   (c) *$\gamma_j \leqslant \gamma_{j-1} - \alpha_{j-1} \leqslant \gamma_0 - j\alpha_0$ for $j = 1, 2, \ldots, N$,*
   (d) *the partition of t_N at most produces a new obtuse triangle t_{N+1}, and at this point no new similarly distinct triangles are generated.*

Proof. The proof of part (2) of this theorem is based on the repetitive use of the inequality of part (1), while the inequality $\gamma_j \leqslant \gamma_0 - j\alpha_0$ implies that after a finite number of steps the new triangle becomes non-obtuse. □

Remark 3.1.

1. Note that the iterative longest-edge bisection of an equilateral triangle t and its descendants produces four similarly distinct triangles, while the 4-triangles longest-edge partition of t and its descendants produces two similarly distinct triangles.
2. Calling T_{QE} the set of quasi-equilateral triangles, namely those triangles that behave as the equilateral triangle with respect to the longest-edge bisection, it is easy to see that for any triangle t_0 in T_{QE}, the 4-triangles longest-edge partition of t_0 and its descendants, produces only two similarly distinct triangles (an obtuse one, and a non-obtuse one both in T_{QE}) with smallest angle greater than or equal to $\alpha_0/2$. Note that this also implies that the triangles of T_{QE} are not small-angled triangles (not far from the equilateral triangle).

By using the concepts involved in the preceding remarks, the following improvement property (see Ref. [24]) holds:

Proposition 3.2. *Let us consider the (global) iterative* 4*-triangles longest-edge partition of t_0 as follows*: *define $T_0 = \{t_0\}$ the triangulation of level* 0, *then the iteration k defines the conforming triangulation T_k at level k, obtained by partition of every triangle in the triangulation of level $k-1$, for $k = 1, 2, \ldots$. Then the percentage of triangles in $T_{QE} \cap T_k$ (and the area of t_0 covered by these triangles) increases as k does.*

The 4T-similar partition produces four triangles similar to its father (see Fig. 3(b)) and has been used in finite element applications [5,1].

Definition 3.5 (*the 2D Baricentric partition*). The baricentric partition of t is defined as follows:

1. Add a new node P at the baricentric point of t, and new nodes at the midpoints of the edges of t.

2. Join the baricentric point P with every vertex and node over the boundary of t (see Fig. 3(c)).

Proposition 3.3. *For the baricentric partition, the number of nodes, edges and triangles of a refined mesh (respectively, N_n, E_n and T_n) are related with the number of elements of the precedent mesh τ_{n-1} by means of the following constitutive equations*:

$$\begin{aligned} N_n &= N_{n-1} + E_{n-1} + T_{n-1}, \\ E_n &= 2E_{n-1} + 6T_{n-1}, \\ T_n &= 6T_{n-1}. \end{aligned} \tag{4}$$

In general any skeleton-regular simplex partition in 2D has an associated set of difference constitutive equations:

$$\begin{aligned} N_n &= N_{n-1} + aE_{n-1} + bT_{n-1}, \\ E_n &= cE_{n-1} + dT_{n-1}, \\ T_n &= eT_{n-1}, \end{aligned} \tag{5}$$

where the parameters a, b, c, d, e are determined by the specific partition and, respectively, correspond to the number of nodes per edge, the number of internal nodes per triangle, the number of son-edges per edge, the number of internal edges per triangle, and the number of son-triangles per triangle. We shall prove that in 2D the asymptotic average adjacencies are independent of these parameters, and hence all the 2D skeleton-regular partitions show the same asymptotic behavior for the average adjacencies.

Remark 3.2.

(1) Both the 4T-similar partition and the baricentric partition do not discriminate between the edges of the triangle. On the contrary the 4T-LE partition distinguishes the longest-edge of the triangle, an important property to design local mesh refinement algorithms [22,23,25].
(2) Note that two different geometric partitions can have the same set of associated difference equations.

4. Skeleton-regular partitions in 3D

In 3D several algorithms have been developed in the last years for refining (and coarsening) tetrahedral meshes. Algorithms based on pure longest-edge bisection (a non-skeleton-regular partition) of tetrahedra have been developed by Rivara and Levin [26], and by Muthukrishnan et al. [16]. The following 8-tetrahedra longest-edge partition was introduced and discussed by Plaza and co-authors [19–21,27].

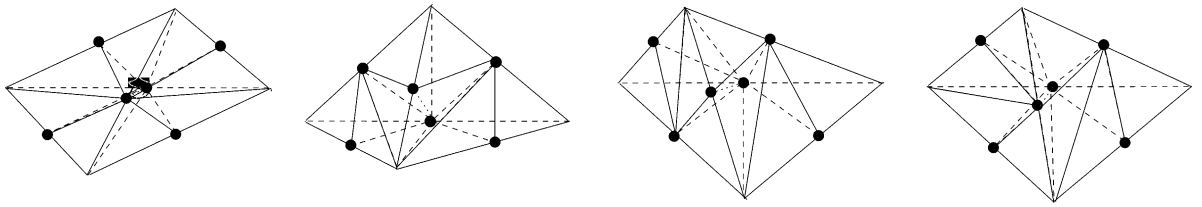

Fig. 4. Refinement patterns for the 8T-LE partition.

Definition 4.1 (*the* 8-*tetrahedra longest-edge* (8*T-LE*) *partition*). For any input tetrahedron t, the 8T-LE partition of t produces eight tetrahedra by performing the 4T-LE partition of the faces of t, and by subdividing the interior of the tetrahedron t consistently with the refined 2-skeleton (see Fig. 4).

This partition was used by Plaza and Carey [19,20] for designing the (3D skeleton-based-refinement) 3D-SBR algorithm.

The 8T-LE partition can be achieved by performing a sequence of bisections by the midpoints of the edges of the original tetrahedron as follows [27]:

Theorem 4.1. *For any tetrahedron t of unique longest-edge, the 8T-LE partition of t is obtained as follows*:

1. *Longest edge bisection of t producing tetrahedra* t_1, t_2.
2. *Bisection of* t_i, *for* $i=1,2$, *by the longest edge of the common face of* t_i *with the original tetrahedron t, producing tetrahedra* t_{ij}, *for* $j=1,2$.
3. *Bisection of each* t_{ij} *by the midpoint of the unique edge equal to an edge of the original tetrahedron.*

Even when there is still no mathematical proof on the creation of a finite number of congruence classes when the 8T-LE partition is applied recursively over an initial triangulation, experimental evidence has been reported in Ref. [27], supporting the conjecture that the partition has a *self-improvement property* in the case of *bad shaped* triangulations, as it happens in 2D [25].

Other tetrahedra partitions have been proposed by Bänsch [2], Kossaczký [13], or Liu and Joe [15]. Although these partitions are not longest-edge based partitions, all of them have associated constitutive difference equations identical to those of the 8T-LE partition, since all divide equal dimension elements in the same number of son-elements. They divide the edges into two edges, the triangular faces into four triangles, and the tetrahedra into eight son-tetrahedra.

The constitutive equations for the 8T-LE partition are the following:

$$\begin{aligned} N_n &= N_{n-1} + E_{n-1} + T_{n-1}, \\ E_n &= 2E_{n-1} + 3F_{n-1} + T_{n-1}, \\ F_n &= 4F_{n-1} + 8T_{n-1}, \\ T_n &= 8T_{n-1}, \end{aligned} \tag{6}$$

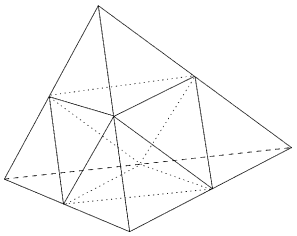

Fig. 5. First step of 3D Freudenthal–Bey partition.

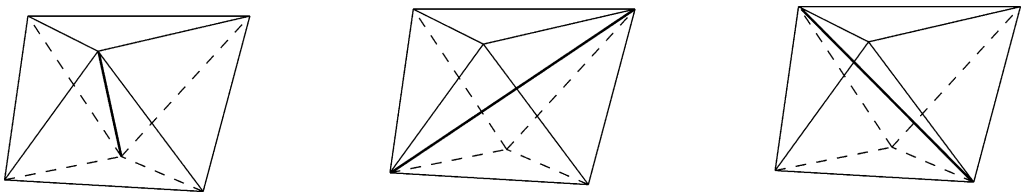

Fig. 6. The three possibilities for dividing the interior octahedron into four tetrahedra.

where N_n, E_n, F_n, and T_n are, respectively, the number of nodes, edges, faces and tetrahedra in the mesh τ_n obtained after n iterative applications of the partition to any initial mesh τ_0.

Definition 4.2 (*the 3D Freudenthal-Bey partition*). For any tetrahedron t, the 3D Freudenthal–Bey partition of t is obtained by firstly cutting off the four corners of t by the midpoints of the edges (Fig. 5) and then by dividing the remaining octahedron according with three patterns associated with the three possible interior diagonals (Fig. 6) [7].

The constitutive equations for the Freudenthal–Bey partition are also Eqs. (6).

Definition 4.3 (*the 3D baricentric partition*). For any tetrahedron t the baricentric partition of t is defined as follows:

1. Add a new node P at the baricentric point of t, add new nodes at the baricentric points of the faces of t, and put new nodes at the midpoint of the edges of t.
2. Perform over each face of t the baricentric triangular partition of the face as shown in Fig. 1(c).
3. Join the baricentric point P with every vertex and node introduced in point (1) (see Fig. 7).

The constitutive equations of the 3D baricentric partition are as follows:

$$\begin{aligned} N_n &= N_{n-1} + E_{n-1} + F_{n-1} + T_{n-1}, \\ E_n &= 2E_{n-1} + 6F_{n-1} + 14T_{n-1}, \\ F_n &= 6F_{n-1} + 36T_{n-1}, \\ T_n &= 24T_{n-1}. \end{aligned} \tag{7}$$

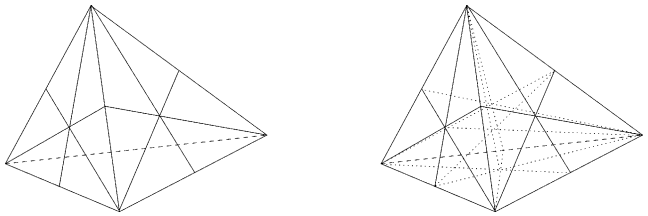

Fig. 7. 3D baricentric partition.

Table 1
Adjacency relations

	2D	3D
Vertices/edge	2	2
Vertices/triangle	3	3
Edges/triangle	3	3
Triangles/edge	2	Not fixed
Vertices/tetrahedron	—	4
Edges/tetrahedron	—	6
Faces/tetrahedron	—	4
Tetrahedra/triangle	—	2
Edges/vertex	Not fixed	Not fixed
Triangles/vertex	Not fixed	Not fixed
Tetrahedra/edge	—	Not fixed
Tetrahedra/vertex	—	Not fixed

5. Adjacency relations in the mesh

Table 1 shows the most important adjacency relations between the topological components of any tetrahedral mesh, and the interior elements in meshes of triangles and tetrahedra.

In other words, the numbers of k-faces of j-simplices, where $k \leqslant j \leqslant n$ are related by the following equation:

$$\#(k\text{-faces}/j\text{-simplex}) = \binom{j+1}{k+1} \quad \text{for } n = 2, 3$$

while that the number of n-simplices by $(n-1)$-faces are summarized by

$$\#n\text{-simplices}/(n-1)\text{-face} = 2.$$

In what follows we shall study the set of remaining non-trivial relations, that is these values in average as well as their asymptotic values when the number of iterative partitions goes to infinity.

Lemma 5.1. *For any 2D conforming triangulation having N_n nodes, E_n edges, and T_n triangles, the average number of triangles by node and edges by node are given as follows*:

$$\text{Av}\#(\textit{triangles per node}) = \frac{3T_n}{N_n},$$

$$\mathrm{Av}\#(\textit{edges per node}) = \frac{2E_n}{N_n}.$$

Proof. Let us consider first the average of triangles per node. Since we are calculating an average per node, the denominator has to be N_n. The numerator in exchange is

$$\sum_{i=1}^{n} n_T(i), \tag{8}$$

where $n_T(i)$ represents the number of triangles sharing node i. However, since this sum is equal to the sum of the number of nodes per triangle, it follows that

$$\sum_{i=1}^{n} n_T(i) = 3T_n. \tag{9}$$

For the average number of edges per node the reasoning is the same. □

Lemma 5.2. *Let τ_0 be any conforming 2D triangulation, and τ_n be the triangulation obtained after n applications of any skeleton-regular partition over each element of the preceding meshes τ_k for $k = 0, 1, 2, \ldots, n-1$. Let N_n, E_n, and T_n be the number of nodes, edges and triangles of τ_n, respectively. Then, the non-trivial adjacency relations in average hold*

$$\lim_{n\to\infty} \mathrm{Av}\#(\textit{triangles per node}) = \lim_{n\to\infty} \mathrm{Av}\#(\textit{edges per node}).$$

Proof. It follows from Lemma 5.1 and the fact that the average number of triangles per edge is $\#(\textit{triangles per edge}) = 2 = \lim_{n\to\infty} 3T_n/E_n$, so $3T_n \sim 2E_n$, and the proof is completed. □

Lemma 5.3. *Let τ_n a 3D triangulation with N_n nodes, E_n edges, F_n faces, and T_n tetrahedra. Then, the non-trivial adjacency relations are*

$$\mathrm{Av}\#(\textit{tetrahedra per edge}) = \frac{6T_n}{E_n},$$
$$\mathrm{Av}\#(\textit{faces per edge}) = \frac{3F_n}{E_n},$$
$$\mathrm{Av}\#(\textit{tetrahedra per node}) = \frac{4T_n}{N_n},$$
$$\mathrm{Av}\#(\textit{faces per node}) = \frac{3F_n}{N_n},$$
$$\mathrm{Av}\#(\textit{edges per node}) = \frac{2E_n}{N_n}.$$

Proof. The argument is the same as in Lemma 5.1. □

Analogously, for the 3D case the following result holds:

Lemma 5.4. *Let τ_0 be a 3D triangulation, and τ_n the triangulation obtained after n iterative global applications of any regular partition. Let N_n, E_n, F_n, and T_n be the number of nodes, edges, faces, and tetrahedra of τ_n, respectively. Then, the non-trivial adjacency relations, in average, verify*:

$$\lim_{n\to\infty} \mathrm{Av}\#(\textit{tetrahedra per edge}) = \lim_{n\to\infty} \mathrm{Av}\#(\textit{faces per edge}),$$

$$\tfrac{1}{2} \lim_{n\to\infty} \mathrm{Av}\#(\textit{tetrahedra per node}) = \tfrac{1}{3} \lim_{n\to\infty} \mathrm{Av}\#(\textit{faces per node}).$$

In order to calculate the asymptotic average adjacencies of the topological components of a particular skeleton-regular partition, we need to solve its associated constitutive equations. This can also be done either by generation functions [12] or by using a symbolic calculus package like MAPLE © [18] or Mathematica ©.

Next we report the results relative to the partitions introduced in Sections 3 and 4.

Theorem 5.1. *Let τ_0 be a (conforming) triangular mesh. For any skeleton-regular partition let N_n, E_n, and T_n be the total number of nodes, edges, and triangles, respectively, after the nth partition application. Then the asymptotic average of non-trivial adjacency numbers (noted as* As Av# *for Asymptotic Average Number of) of topological elements are independent of the particular partition of each triangle and these numbers are as follows*:

$$\text{As Av}\#(\textit{triangles per node}) = \lim_{n\to\infty} \frac{3T_n}{N_n} = 6,$$

$$\text{As Av}\#(\textit{edges per node}) = \lim_{n\to\infty} \frac{2E_n}{N_n} = 6.$$

Proof. The constitutive Eqs. (5) associated to a general skeleton-regular partition in a 2D triangulation can be written in matrix form as follows:

$$u_n = \begin{pmatrix} N_n \\ E_n \\ T_n \end{pmatrix} = \begin{pmatrix} 1 & a & b \\ 0 & c & d \\ 0 & 0 & e \end{pmatrix} \begin{pmatrix} N_{n-1} \\ E_{n-1} \\ T_{n-1} \end{pmatrix} = A u_{n-1} \tag{10}$$

So, applying the former equation to u_{n-1}, and so on, we obtain:

$$u_n = A^2 u_{n-2} = \cdots = A^n u_0 = A^n \begin{pmatrix} N_0 \\ E_0 \\ T_0 \end{pmatrix}, \tag{11}$$

where N_0, E_0, and T_0 are the initial values for the number of nodes, edges and triangles, respectively. Note that matrix A is non-singular since $c = \#(\text{edges per edge}) \geqslant 1$, and $e = \#(\text{triangles per triangle}) > 1$. Furthermore, $d > 0$, and consequently $e > c$ since counting the number of edges after one application of the partition to a single triangle we obtain $3e = 3c + 2d$, so $3(e - c) = 2d > 0$.

So, if $c > 1$, since $e > c$, then matrix A defining the constitutive equation is diagonalizable. Otherwise, if $c = 1$, then $a = 0$ and matrix A can be written as

$$A = \begin{pmatrix} 1 & 0 & b \\ 0 & 1 & d \\ 0 & 0 & e \end{pmatrix} = \begin{pmatrix} -\frac{-e+1+b}{e-1} & \frac{b}{e-1} & 1 \\ -\frac{d}{e-1} & \frac{d}{e-1} & 0 \\ 0 & 1 & 0 \end{pmatrix} \begin{pmatrix} 1 & 0 & 0 \\ 0 & e & 0 \\ 0 & 0 & 1 \end{pmatrix} \begin{pmatrix} 0 & -\frac{e-1}{d} & 1 \\ 0 & 0 & 1 \\ 1 & -\frac{-e+1+b}{d} & -1 \end{pmatrix}.$$

Therefore, we can apply the classical result that states that if A is a diagonalizable matrix ($A = SDS^{-1}$, D being a diagonal matrix and S non-singular matrix) $A^n = SD^nS^{-1}$ [30]. Then we get the following value for u_n:

$$u_n = \begin{pmatrix} N_n \\ E_n \\ T_n \end{pmatrix} = \begin{pmatrix} (1 + \frac{1}{2}(1 + 3a + 2b)^n - \frac{3}{2}(a+1)^n)T_0 + (-1 + (a+1)^n)E_0 + N_0 \\ (\frac{3}{2}(1 + 3a + 2b)^n - \frac{3}{2}(a+1)^n)T_0 + (a+1)^n E_0 \\ (1 + 3a + 2b)^n T_0 \end{pmatrix}.$$

Once the recurrence equations have been solved, taking limits in the quotients we obtain:

$$\lim_{n\to\infty} \frac{3T_n}{N_n} = \lim_{n\to\infty} \frac{3(1 + 3a + 2b)^n T_0}{(1 + 1/2(1 + 3a + 2b)^n - 3/2(a+1)^n)T_0 + (-1 + (a+1)^n)E_0 + N_0}$$

$$= \lim_{n\to\infty} \frac{3(1 + 3a + 2b)^n T_0}{(1/2(1 + 3a + 2b)^n)T_0} = 6,$$

$$\lim_{n\to\infty} \frac{2E_n}{N_n} = \lim_{n\to\infty} \frac{2(3/2(1 + 3a + 2b)^n - 3/2(a+1)^n)T_0 + (a+1)^n E_0}{(1 + 1/2(1 + 3a + 2b)^n - 3/2(a+1)^n)T_0 + (-1 + (a+1)^n)E_0 + N_0}$$

$$= \lim_{n\to\infty} \frac{2(3/2(1 + 3a + 2b)^n)T_0}{(1/2(1 + 3a + 2b)^n)T_0} = 6. \qquad \square$$

In 3D different asymptotic values are obtained in general for different partitions, as shown below for the partitions of Section 4.

Theorem 5.2. *Let τ be a (conforming) initial tetrahedral mesh in which the 8T-LE partition is recursively applied. Then the asymptotic average non-trivial adjacencies are the following*:

$$\text{As Av\#}(\textit{tetrahedra per edge}) = \lim_{n\to\infty} \frac{6T_n}{E_n} = \frac{36}{7},$$

$$\text{As Av\#}(\textit{tetrahedra per node}) = \lim_{n\to\infty} \frac{4T_n}{N_n} = 24,$$

$$\text{As Av\#}(\textit{faces per edge}) = \lim_{n\to\infty} \frac{3F_n}{E_n} = \frac{36}{7},$$

$$\text{As Av\#}(\textit{faces per node}) = \lim_{n\to\infty} \frac{3F_n}{N_n} = 36,$$

$$\text{As Av\#}(\textit{edges per node}) = \lim_{n\to\infty} \frac{2E_n}{N_n} = 14.$$

Proof. Note first that the constitutive Eqs. (6) for the 8T-LE partition can also be written in matrix form as

$$u_n = \begin{pmatrix} N_n \\ E_n \\ F_n \\ T_n \end{pmatrix} = \begin{pmatrix} 1 & 1 & 0 & 0 \\ 0 & 2 & 3 & 1 \\ 0 & 0 & 4 & 8 \\ 0 & 0 & 0 & 8 \end{pmatrix} \begin{pmatrix} N_{n-1} \\ E_{n-1} \\ F_{n-1} \\ T_{n-1} \end{pmatrix} = Au_{n-1}, \tag{12}$$

where matrix A is diagonalizable

$$A = \begin{pmatrix} 1 & 1 & 0 & 0 \\ 0 & 2 & 3 & 1 \\ 0 & 0 & 4 & 8 \\ 0 & 0 & 0 & 8 \end{pmatrix} = SDS^{-1}$$

$$= \begin{pmatrix} -\frac{4}{3} & \frac{7}{3} & -\frac{7}{6} & \frac{7}{6} \\ 0 & \frac{7}{3} & -\frac{7}{2} & \frac{7}{6} \\ 0 & 0 & -\frac{7}{3} & 2 \\ 0 & 0 & 0 & 1 \end{pmatrix} \begin{pmatrix} 1 & 0 & 0 & 0 \\ 0 & 2 & 0 & 0 \\ 0 & 0 & 4 & 0 \\ 0 & 0 & 0 & 8 \end{pmatrix} \begin{pmatrix} -\frac{3}{4} & \frac{3}{4} & -\frac{3}{4} & \frac{3}{4} \\ 0 & \frac{3}{7} & -\frac{9}{14} & \frac{11}{14} \\ 0 & 0 & -\frac{3}{7} & \frac{6}{7} \\ 0 & 0 & 0 & 1 \end{pmatrix}.$$

Then, since $u_n = A^n u_0$ the constitutive equations can be easily solved and we obtain:

$$\begin{pmatrix} N_n \\ E_n \\ F_n \\ T_n \end{pmatrix} = \begin{pmatrix} (\frac{1}{6}8^n - 4^n + \frac{11}{6}2^n - 1)T_0 + (1 - \frac{3}{2}2^n + \frac{1}{2}4^n)F_0 + (-1 + 2^n)E_0 + N_0 \\ (\frac{7}{6}8^n - 34^n + \frac{11}{6}2^n)T_0 + (-\frac{3}{2}2^n + \frac{3}{2}4^n)F_0 + 2^n E_0 \\ (28^n - 24^n)T_0 + 4^n F_0 \\ 8^n T_0 \end{pmatrix},$$

where N_0, E_0, F_0, and T_0 are the number of nodes, edges, faces and tetrahedra in the initial triangulation. Taking limits in the appropriate quotients as in Theorem 5.2 we obtain the asymptotic average adjacencies. □

Remark 5.1. Since the 3D Freudenthal–Bey partition is equivalent in average to the 8T-LE partition, both have the same asymptotic average adjacencies.

Theorem 5.3. *Let τ be a (conforming) initial tetrahedral mesh in which the baricentric partition is recursively applied. Then the asymptotic average adjacencies are the following*:

$$\text{As Av\#}(\textit{tetrahedra per edge}) = \lim_{n\to\infty} \frac{6T_n}{E_n} = \frac{66}{13},$$

$$\text{As Av\#}(\textit{tetrahedra per node}) = \lim_{n\to\infty} \frac{4T_n}{N_n} = 22,$$

$$\text{As Av\#}(\textit{faces per edge}) = \lim_{n\to\infty} \frac{3F_n}{E_n} = \frac{66}{13},$$

$$\text{As Av\#}(\textit{faces per node}) = \lim_{n\to\infty} \frac{3F_n}{N_n} = 33,$$

$$\text{As Av\#}(\textit{edges per node}) = \lim_{n\to\infty} \frac{2E_n}{N_n} = 13.$$

Remark 5.2. Note, that although all the triangle partitions show the same asymptotic behavior for their average adjacencies, not all of them have the non-degeneracy properties of the longest-edge based partitions (Theorems 3.1 and 3.2). To see this, consider the 3-triangles partition defined by putting one interior node at the baricenter of each triangle and then joining this node with the three nodes of the triangle. This partition degenerates, since the smallest angle tends to zero when the partition is repeatedly used over any triangle and its descendants.

In 3D the non-degeneracy properties of both the longest-edge partition and the 8-tetrahedra longest-edge based partition, and the respective local refinement algorithms have not been reported yet.

6. Empirical results

In this section, we report evidence that supports the conjecture on the non-degeneracy property of both the 8T-LE partition and the mesh refinement algorithms based on this partition.

Here three numerical examples are presented. In every case, the 8T-LE partition has been applied seven times to an initial tetrahedron and its descendants, so the last level of division (τ_8) contains 366,145 vertices and 2,097,152 tetrahedra. For each test tetrahedron a set of three tables have been produced: the first one contains the coordinates of the vertices, while that the second and third ones summarize statistical information for the meshes obtained.

The values $\Phi_T, \Phi_{\min}$ and $\Phi_{\max}$ expressed in sexagesimal degrees, refer to the solid angle measure (Φ_P) used by Rivara and Levin [26] and defined, at each vertex P as follows:

$$\Phi_P = \sin^{-1}\{(1 - \cos^2\alpha_P - \cos^2\beta_P - \cos^2\gamma_P + 2\cos\alpha_P\cos\beta_P\cos\gamma_P)^{1/2}\}, \tag{13}$$

where α_P, β_P, and γ_P are the three planar angles sharing vertex P.

Φ_T is the minimum Φ-value for the solid angles of tetrahedron T, and $\Phi_{\min}$ and $\Phi_{\max}$ are, respectively, equal to the minimum and maximum Φ-values attained for the mesh at level n. Note that $0 \leqslant \Phi_T \leqslant 45$, and $\Phi = 0$ implies a totally degenerate tetrahedron. (For a discussion on tetrahedron shape measures see, for example [14].)

Note that the solid angle at P, say Ω_P, can be calculated from the following formula [14,19] as a function of the planar angles at P:

$$\sin(\Omega_P/2) = \frac{(1 - \cos^2\alpha_P - \cos^2\beta_P - \cos^2\gamma_P + 2\cos\alpha_P\cos\beta_P\cos\gamma_P)^{1/2}}{4\cos(\alpha_P/2)\cos(\beta_P/2)\cos(\gamma_P/2)}. \tag{14}$$

In the first test problem the initial tetrahedron is a right-tetrahedron, with a vertex in the origin of the coordinate system, and three vertices over the axes of the coordinate system to equal distance from the origin (see Table 2). The evolution of the shape for the tetrahedra as the partition proceeds is in Table 3. Since the element improvement is relative to the shape quality of the input tetrahedron, an element T is assumed to be bad-shaped if its minimum solid angle associated measure verifies $\Phi_T < 10$ for the test problems 1 and 3, while that for the test problem 2 it is assumed $\Phi_T < 0.24$ for bad-shaped tetrahedra. Note that the minimum solid angle remains constant since the second global partition, while the percentage of volume covered by bad-shaped elements improves from the third global partition.

Table 2
Vertices (Test problem 1—right-shaped tetrahedron)

0.0	0.0	0.0
4.0	0.0	0.0
0.0	4.0	0.0
0.0	0.0	4.0

Table 3
Evolution of shape (Test problem 1—right-shaped tetrahedron)

Level	Num. of nodes	Num. of elems.	$\Phi_{\min}$	Planar angles	$\Phi_{\max}$	% of bad elems. ($\Phi_T < 10$)	% volume covered by bad elems.
1	4	1	30.00	45.00 # 60.00 # 45.00	90	0.00	0.00
2	10	8	9.59	19.47 #35.26 # 30.00	90	25.00	25.00
3	35	64	9.59	30.00 #35.26 # 19.47	90	25.00	25.00
4	165	512	9.59	30.00 #35.26 # 19.47	90	20.31	20.31
5	969	4096	9.59	30.00 #35.26 # 19.47	90	15.62	15.62
6	6545	32,768	9.59	30.00 #35.26 # 19.47	90	11.82	11.82
7	47,905	262,144	9.59	30.00 #35.26 # 19.47	90	8.89	8.89
8	366,145	2,097,152	9.59	30.00 #35.26 # 19.47	90	6.67	6.67

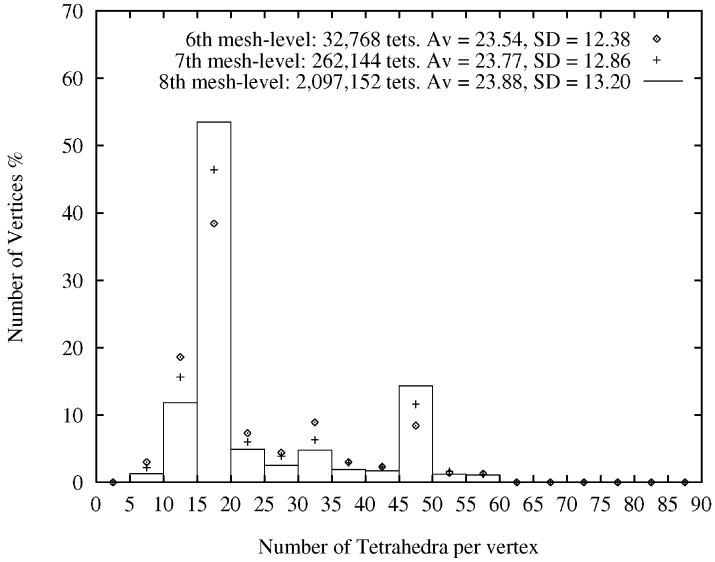

Fig. 8. Distribution of vertices versus number of tetrahedra per vertex. Right-shaped tetrahedron.

Figs. 8–10 show the evolution of the numbers of tetrahedra per vertex as the global refinement (partition) proceeds. Note that the distribution tends to concentrate more tetrahedra per node around 24, which is the asymptotic average number for this partition.

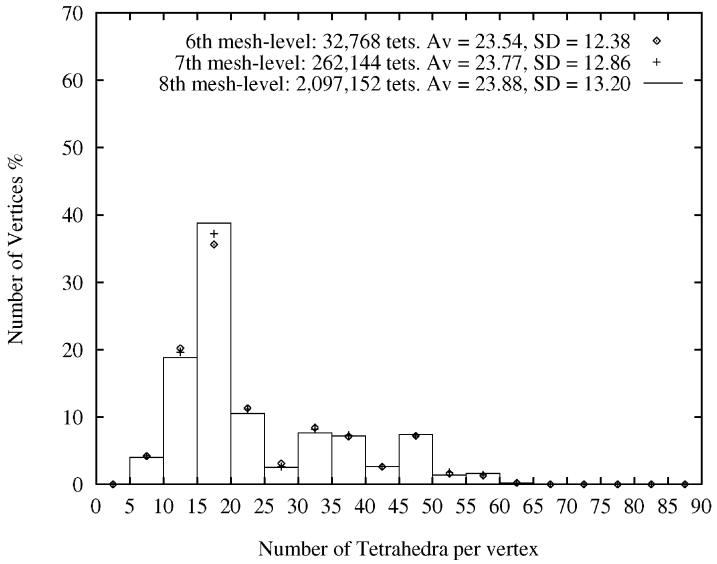

Fig. 9. Distribution of vertices versus number of tetrahedra per vertex. Needle tetrahedron.

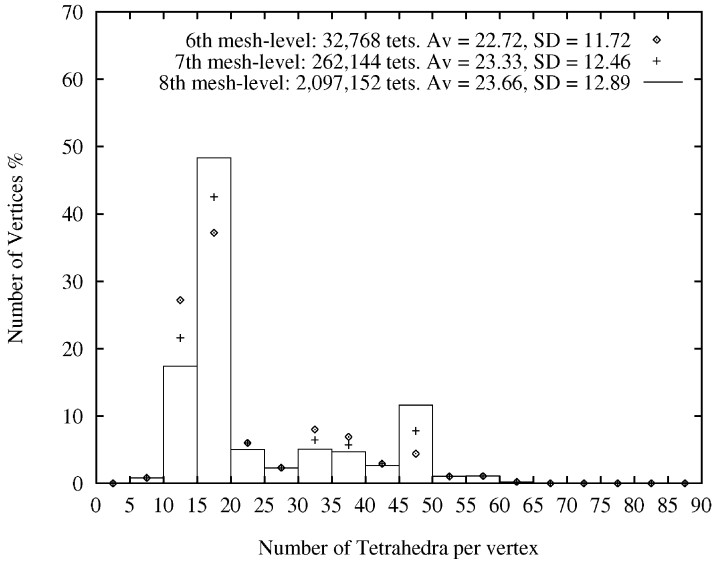

Fig. 10. Distribution of vertices versus number of tetrahedra per vertex. Flat tetrahedron.

The second example considers a needle tetrahedron (see Table 4). Table 5 shows the evolution of the minimum and maximum angles, and the % of volume covered by bad-shaped elements, while Fig. 9 shows the evolution of tetrahedra per node for this needle tetrahedron. Note that in this case the distribution also approaches the mean value 24.

Table 4
Vertices (Test problem 2—Needle tetrahedron)

−0.5	0.0	0.0
0.5	0.0	0.0
0.0	0.2	0.0
0.0	0.0	7.0

Table 5
Evolution of shape (Test problem 2—Needle tetrahedron)

Level	Num. of nodes	Num. of elems.	$\Phi_{\min}$	Planar angles	$\Phi_{\max}$	% of bad elems. ($\Phi_T < 0.24$)	% volume covered by bad elems.
1	4	1	0.23	8.00 # 4.36 # 4.28	43.58	100.00	100.00
2	10	8	0.23	8.00 # 4.26 # 4.28	67.84	75.00	75.00
3	35	64	0.22	4.26 # 4.36 # 8.00	68.14	68.75	68.75
4	165	512	0.22	4.28 # 4.36 # 8.01	68.14	67.19	67.19
5	969	4096	0.22	4.23 # 4.35 # 7.96	68.14	66.80	66.80
6	6545	32,768	0.22	4.23 # 4.35 # 7.96	68.14	66.71	66.71
7	47,905	262,144	0.22	7.96 # 4.23 # 4.35	68.14	66.63	66.63
8	366,145	2,097,152	0.22	7.96 # 4.23 # 4.35	68.14	66.63	66.63

Table 6
Vertices (Test problem 3—flat tetrahedron)

−2.0	0.0	0.0
4.0	0.0	0.0
1.3	3.5	0.0
1.0	1.3	0.5

The third example corresponds to a flat tetrahedron (Table 6). Table 7 shows for this example the evolution of the shape of the elements and meshes obtained at global partitioning. Note that the minimum solid angle remains constant since the second global refinement, while the percentage of volume covered by bad-shaped tetrahedra improves when the partitioning proceeds.

Table 8 shows the evolution of the average number of tetrahedra per vertex, and the standard deviation for the distribution of tetrahedra per vertex for the last example, in the first seven stages of application of the 8T-LE partition.

Remark 6.1 (a comparison on Beall and Shephard estimates). Beall and Shephard [3,4] have estimated numbers of nodes, edges, faces and tetrahedra in the meshes used in finite element calculations as follows:

$$\text{Av\#}(\textit{tetrahedra per edge}) = 5,$$
$$\text{Av\#}(\textit{tetrahedra per node}) = 23,$$
$$\text{Av\#}(\textit{faces per edge}) = 5,$$

Table 7
Evolution of shape (Test problem 3—Flat tetrahedron)

Level	Num. of nodes	Num. of elems.	$\Phi_{\min}$	Planar angles	$\Phi_{\max}$	% of bad elems. ($\Phi_T < 10$)	% volume covered by bad elems.
1	4	1	6.31	24.90 # 24.74 # 46.78	24.94	100.00	100.00
2	10	8	3.68	40.11 # 6.08 # 38.42	33.30	62.50	62.50
3	35	64	3.12	46.68 # 27.74 # 19.70	75.29	45.31	45.31
4	165	512	3.12	46.68 # 27.74 # 19.70	75.29	37.50	37.50
5	969	4096	3.12	46.68 # 27.74 # 19.70	75.29	30.03	30.03
6	6545	32,768	3.12	46.68 #27.74 #19.70	75.29	22.97	22.97
7	47,905	262,144	3.12	46.68 # 27.74# 19.70	75.29	17.13	17.13
8	366,145	2,097,152	3.12	19.70#46.78# 27.74	74.85	12.57	12.57

Table 8
Statistical measures

Level n	Num. tets.	Av#(tetrahedra per node)
4	512	12.41
5	4.096	16.90
6	32.768	20.03
7	262.144	21.88
8	2.097.152	22.91
9	16.777.216	23.45
10	134.217.728	23.72

$$\text{Av\#}(\textit{faces per node}) = 35,$$
$$\text{Av\#}(\textit{edges per node}) = 14.$$

To compute this estimation an equilateral mesh is assumed, which is known is impossible in 3D, but good for the purposes of determining memory storage requirements. Thus, for example in the case of Av#(tetrahedra per node), the ratio between the value of the solid angle of the full sphere around a vertex and the value of the solid angle of a regular tetrahedron is computed (equal to 22.6 rounded to 23). The other adjacency numbers for the tetrahedral mesh were calculated in a similar way. These numbers were then checked with various practical meshes to make sure that they were sufficiently representative for their purposes. Note that, these numbers, although obtained in a different way and for another purpose than ours, are in the same range that the asymptotic average numbers reported in this paper.

7. Concluding remarks

In this paper, we present a general class of partitions, the skeleton-regular partitions. The asymptotic average adjacencies for skeleton-regular triangular and tetrahedral partitions are studied by solving the recurrence equations characterizing these partitions. We prove that the asymptotic number

of average adjacencies is identical for each 2D skeleton-regular partition, while that in 3D different values are obtained for each 3D partition. This study can be applied to other polyhedral or polygonal partitions of the space, not only simplicial partitions.

Furthermore, empirical experimentation on the practical behavior of the 8T-LE partition has shown that, in general, the minimum solid angle stabilizes in the second or third global iterative partition, while that the percentage of better tetrahedra tends to improve as the refinement proceeds.

Theoretical research in course on the nondegeneracy properties of the 3D longest-edge based partitions will be published elsewhere.

Acknowledgements

The work of the first author and the second author have been, respectively, supported by Project PI-1999/146 from Gobierno de Canarias, and FONDECYT 1981033 from Chile.

References

[1] R.E. Bank, A.H. Sherman, A. Weiser, Refinement Algorithm and Data Structures for Regular Local Mesh Refinement, Scientific Computing, Amsterdam, 1983, pp. 3–17.
[2] E. Bänsch, Local mesh refinement in 2 and 3 dimensions, IMPACT Comput. Sci. Eng. 3 (1991) 181–191.
[3] M.W. Beall, M.S. Shephard, A general topology-based data structure, Internat. J. Numer. Methods Eng. 40 (1997) 1573–1596.
[4] M.W. Beall, M.S. Shephard, Personal communication, 23 July 1999.
[5] E.B. Becker, G.F. Carey, J.T. Oden, Finite Elements, Prentice-Hall, New York, 1981.
[6] M. Berger, Geometry, Springer, New York, 1987.
[7] J. Bey, Simplicial grid refinement: on Freudenthal's algorithm and the optimal number of congruence classes, Numer. Math. 85 (1) (2000) 1–29.
[8] J.F. Buss, R.B. Simpson, Planar mesh refinement cannot be both local and regular, Numer. Math. 79 (1998) 1–10.
[9] G.F. Carey, Computational Grids: Generation, Refinement and Solution Strategies, Taylor & Francis, London, 1997.
[10] L.A. Freitag, Tetrahedral mesh improvement using swapping and smoothing, Internat. J. Numer. Methods Eng. 40 (1997) 3979–4002.
[11] W.H. Frey, D.A. Field, Mesh relaxation: a new technique for improving triangulations, Internat. J. Numer. Methods Eng. 31 (1991) 1121–1133.
[12] R.L. Graham, D.E. Knuth, O. Patashnik, Concrete Mathematics, Addison-Wesley, Reading, MA, 1989.
[13] I. Kossaczký , A recursive approach to local mesh refinement in two and three dimensions, J. Comput. Appl. Math. 55 (1994) 275–288.
[14] A. Liu, B. Joe, On the shape of tetrahedra from bisection, Math. Comput. 63 (1994) 141–154.
[15] A. Liu, B. Joe, Quality local refinement of tetrahedral meshes based on bisection, SIAM J. Sci. Statist. Comput. 16 (1995) 1269–1291.
[16] M.C. Muthukrishnan, P.S. Shiakolas, R.V. Nambiar, K.L. Lawrence, Simple algorithm for Adaptive Refinement of three-dimensional finite element tetrahedral meshes, AIAA J. 33 (1995) 928–932.
[17] J. Pach, New trends in discrete and computational geometry, Springer, Berlin, 1993.
[18] A. Plaza, Asymptotic behavior of the average adjacencies of the topological elements in some simplex partitions, Proceedings of the 8th International Meshing Roundtable, South Lake Tahoe, 1999, pp. 233–240.
[19] A. Plaza, G.F. Carey, A new refinement algorithm for tetrahedral grids based on bisection, TICAM Tech. Rep., 96/54, U.T. at Austin, 1996.
[20] A. Plaza, G.F. Carey, Refinement of simplicial grids based on the skeleton, Appl. Numer. Math. 32 (2) (2000) 195–218.

[21] A. Plaza, M.A. Padrón, G.F. Carey, A 3D refinement/derefinement combination to solve evolution problems, Appl. Numer. Math. 32 (4) (2000) 401–418.
[22] M.C. Rivara, Mesh refinement based on the generalized bisection of simplices, SIAM J. Numer. Anal. 2 (1984) 604–613.
[23] M.C. Rivara, Selective refinement/derefinement algorithms for sequences of nested triangulations, Internat. J. Numer. Methods Eng. 28 (1989) 2889–2906.
[24] M.C. Rivara, G. Iribarren, The 4-triangles longest-side partition of triangles and linear refinement algorithms, Math. Comput. 65 (1996) 1485–1502.
[25] M.C. Rivara, New longest-edge algorithms for the refinement and/or improvement of unstructured triangulations, Internat. J. Numer. Meth. Eng. 40 (1997) 3313–3324.
[26] M.C. Rivara, C. Levin, A 3D refinement algorithm suitable for adaptive and multigrid techniques, Comm. Appl. Numer. Methods Eng. 8 (1992) 281–290.
[27] M.C. Rivara, A. Plaza, Mesh refinement/derefinement based on the 8-tetrahedra longest-edge partition, Department of Computer Science, U. de Chile, TR/DCC-99-6, 1999.
[28] M.C. Rivara, M. Venere, Cost analysis of the longest-side (triangle bisection) refinement algorithm for triangulations, Eng. Comput. 12 (1996) 224–234.
[29] K. Shimada, Physically-based mesh generation: automated triangulation of surfaces and volumes via bubbles packing, Ph.D. Thesis, MIT, Cambridge, MA, 1993.
[30] G. Strang, Linear Algebra, Academic Press, Inc., New York, 1976.